





[View Journal Online](#)  
[View Article Online](#)

## Theoretical study of the paracetamol adsorption over a graphene oxide sheet

Beatriz Paulina López-Jesús <sup>1</sup>, Sandy María Pacheco-Ortín <sup>1,2</sup> and Esther Agacino-Valdés <sup>1,2,\*</sup><sup>1</sup> Centro de Investigaciones Teóricas, Facultad de Estudios Superiores Cuautitlán, Universidad Nacional Autónoma de México, Cuautitlán Izcalli, CP 54740, Estado de México, México<sup>2</sup> Departamento de Química, Facultad de Estudios Superiores Cuautitlán, Universidad Nacional Autónoma de México, Cuautitlán Izcalli, CP 54740, Estado de México, México\* Corresponding author at: Centro de Investigaciones Teóricas, Facultad de Estudios Superiores Cuautitlán, Universidad Nacional Autónoma de México, Cuautitlán Izcalli, CP 54740, Estado de México, México.  
e-mail: [agacino@unam.mx](mailto:agacino@unam.mx) (E. Agacino-Valdés).

## RESEARCH ARTICLE



doi: 10.5155/eurjchem.16.4.395-402.2718

Received: 19 September 2025

Received in revised form: 29 October 2025

Accepted: 9 November 2025

Published online: 31 December 2025

Printed: 31 December 2025

## KEYWORDS

Graphene  
Paracetamol  
Graphene oxide  
Water pollution  
DFT calculations  
Adsorption study

## ABSTRACT

In recent decades, the detection of non-steroidal anti-inflammatory drugs (NSAIDs) in various water bodies has raised concerns for their environmental impact, since conventional wastewater treatment plants are inefficient for removing these pharmaceutical contaminants. In this way, many researchers have proposed various techniques, including the use of adsorbent materials. In this work, we conducted a theoretical study of the adsorption of the paracetamol (PCT) molecule on a large cluster ( $C_{80}H_{26}O_{24}$ ) of graphene oxide (GO) that simulates a sheet. The calculations were based on the DFT formalism using the combination M06-2X/6-31G\*\*. The GO sheet used, with a C/O ratio of 3.5 and an oxygen content of 17%, exhibited a high adsorption capacity and stability. The adsorption energies for the most preferred complexes were 22 kcal/mol with adsorption distances between 1.84 and 2.60 Å, which allowed us to conclude that this is a very favored chemisorption process. The interaction distances and adsorption energies obtained were compared with those from other studies, confirming that the DFT approach used in this work, as well as the GO sheet modeled, were suitable. The percentages of elongation of the bonds in the PCT molecule, calculated from the bond distances before and after the adsorption process, evidenced a weakening of certain bonds in the molecule related to its most likely fragmentations. Therefore, it is concluded that these adsorption processes mediated by GO sheets can help, together with other methods, with PCT degradation.

Cite this: *Eur. J. Chem.* 2025, 16(4), 395-402Journal website: [www.eurjchem.com](http://www.eurjchem.com)

## 1. Introduction

Currently, one of the most commonly addressed environmental problems worldwide is water pollution. Recently, chemical products of daily use have been detected in water bodies and effluents from wastewater treatment plants (WWTPs), which were not designed to remove these substances. Although they have been detected at low concentrations, these chemical products have adverse effects on marine fauna and human health [1,2].

Among these substances, pharmaceutical waste, and in particular non-steroidal anti-inflammatory drugs (NSAIDs), have been classified as 'emerging contaminants' (EC) [3], due to the urgency to search for ways to degrade or mineralize them. NSAIDs constitute a heterogeneous group of drugs with analgesic, antipyretic, and anti-inflammatory properties; This group of drugs includes more than 100 compounds and are known to be widely used around the world [4]. These products generate considerable waste, leading to their accumulation in water reservoirs [5]. In particular, the paracetamol molecule (PCT), also known as acetaminophen, is one of the most widely used analgesics worldwide; when ingested, this drug cannot be fully metabolized and approximately 20% of the drug is

excreted into the environment as metabolites, ending up in water bodies and effluent treatment plants [6]. Due to its excessive usage and consumption, PCT has been detected in concentrations ranging from 0.1 to 300 mg/L in effluents and 0.4 to 71 ng/L in rivers [7]; therefore, the removal of PCT and its metabolites/degradation products from wastewater, prior to their discharge into the environment, is mandatory to preserve environmental quality and to avoid their harmful health effects on living beings [8]. In Mexico and Latin America, although few studies have been conducted, pharmaceutical waste has been detected at levels comparable to those reported in Europe and, in some cases, above the limits allowed by environmental regulations, raising concerns about its ecological impact and possible adverse effects on human health [9,10].

Since the conventional techniques used in WWTPs are inefficient for removing pharmaceutical residues, many researchers have proposed and tested various methods based on advanced oxidation processes [11], photocatalysis and UV photolytic techniques [12] or the combination of both techniques, like UV/H<sub>2</sub>O<sub>2</sub>, also called hybrid methodologies [13].

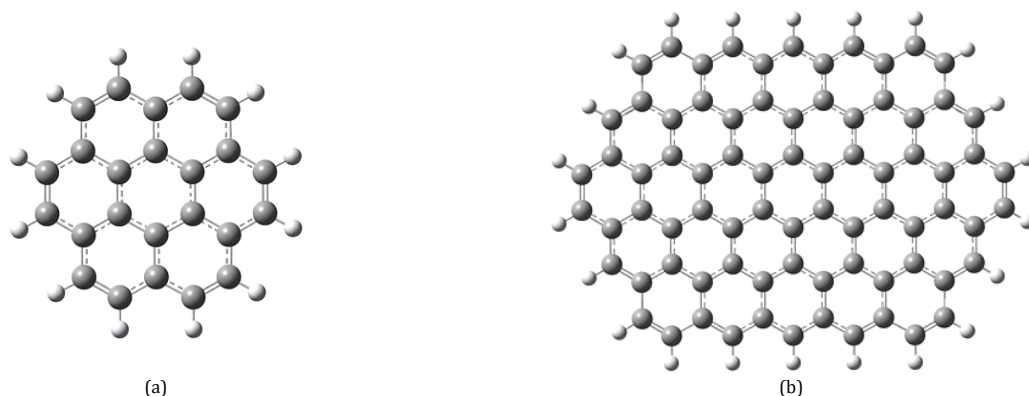


**Figure 1.** Optimized geometry of (a) coronene molecule ( $C_{24}H_{12}$ ) and (b) polycircumcoronene sheet ( $C_{78}H_{22}$ ).

Recently, the use of carbon-based adsorbent materials, such as activated carbon, graphene (G) and graphene oxide (GO), has also been considered [14,15]. Carbon-based materials have always attracted special attention among researchers due to their outstanding physical, chemical and surface properties, which are being applied to the removal of ECs [16]. In particular, one of the key advantages of using graphene oxide in the remediation of emerging contaminants is its ability to remove a wide range of substances, including pharmaceuticals [17]. GO is the oxidized form of graphene and contains various functional groups, such as hydroxyl, carboxyl, and epoxy groups. They act as active sites and anchor points where contaminants will be adsorbed [18,19]. GO has been shown to be very useful in degrading the PCT molecule when combined with other photocatalytic [20] and electrochemical processes [21], when functionalized with semiconductor materials ( $TiO_2$  and  $ZnO$ ) [22] or when decorated with oxides of transition metals such as Fe [23]. Considering the heterogeneity of the GO surface as a result of the functional groups present, we analyze the role of these groups in the adsorption of PCT through a theoretical study using DFT formalism and certain adsorption process descriptors.

## 2. Experimental

### 2.1. Computational details

Calculations were carried out applying the formalism of the density functional theory included in the Gaussian 09 package [24]. The calculation route considered the combination of the density functional and the basis set M06-2X/6-31G\*\*. The hybrid meta-GGA exchange-correlation functional M06-2X [25] has been recommended in several applications, ranging from conjugated polyenes and non-covalent interactions to thermodynamic calculations, making it an excellent alternative for accurately describing dispersion interactions and chemisorption processes of organic molecules on the surface of graphene-based adsorbents [26,27]. On the other hand, the 6-31G\*\* basis set is suitable for calculations on medium-to-large-sized molecules [28], and some studies have shown that its combination with the M06-2X functional provides reliable and accurate results at minimal computational cost [29-31]. This combination offers a reasonable balance between precision and computational costs, which is ideal for medium-sized molecular systems, such as the adsorption complexes studied in this work.

### 2.2. Methodology

In the first stage, the optimizations were carried out in the gas phase, and in the second stage, the Solvation Model Density (SMD) [32] was considered. SMD is a continuum solvation

model based on the charge density of a solute molecule interacting with a solvent, which is described as a dielectric medium with a surface tension value at the solute-solvent boundary. For both phases, the frequency analyses confirmed that the calculated stationary points were truly minima on the potential energy surface (PES). Inclusion of the solvent effect is required because it provides a more realistic representation of the problem under study, specifically the presence of contaminants in water sources, allowing more precise results compared to gas phase calculations [31,33]. The SMD model is widely used in the study of various types of solutes and solvents, and along with the 6-31G\* basis, errors less than 1 kcal/mol have been obtained for the calculation of solvation parameters, using functionals from the same series as the M06-2X; therefore, it was chosen to perform this study [26].

GO sheet modeling is based on a coronene molecule ( $C_{24}H_{12}$ , Figure 1a); this strategy has been employed in many previous works, demonstrating that it can be considered a suitable model for studying these processes [29,33,34]. Since the PCT is a drug with an approximate length of 8.86 Å, the coronene molecule was expanded to form a cluster of polycircumcoronene with 78 carbon atoms in a rectangular shape, as shown in Figure 1b. The GO sheet contributed to the best arrangement of the PCT molecule over the GO sheet. Finally, as Figure 1b shows, hydrogen atoms were added to the carbons located at the cluster periphery to saturate their valences and neutralize possible edge effects; to obtain the GO sheet, this last cluster was functionalized according to certain criteria, which will be explained in the next section.

This study includes the calculation of the energy and adsorption distance of the adsorption complexes GO-PCT as well as the HOMO-LUMO orbital maps, the HOMO-LUMO energy gap, and the molecular electrostatic potential (MEP). In addition, the reactivity of the free GO sheet and PCT molecule was also analyzed using HOMO-LUMO orbital maps and the molecular electrostatic potential (MEP).

## 3. Results and discussion

### 3.1. Modeling of the graphene oxide sheet

The pristine graphene sheet shown in Figure 1b was functionalized considering that on one side, named the main side, there is a combination of epoxide and hydroxyl groups at the center and a combination of carbonyl, hydroxide, and carboxyl groups at the edge, as in the Lerf-Klinowski model [35,36], which was supported by  $^{13}C$  and  $^1H$  NMR studies. Based on this criterion, three different models were explored in which the composition was varied based on the C/O ratio, the oxygen percentage, the OH/epoxy ratio at the center of the main side and the OH/ $CO_2H$  ratio at the edge.

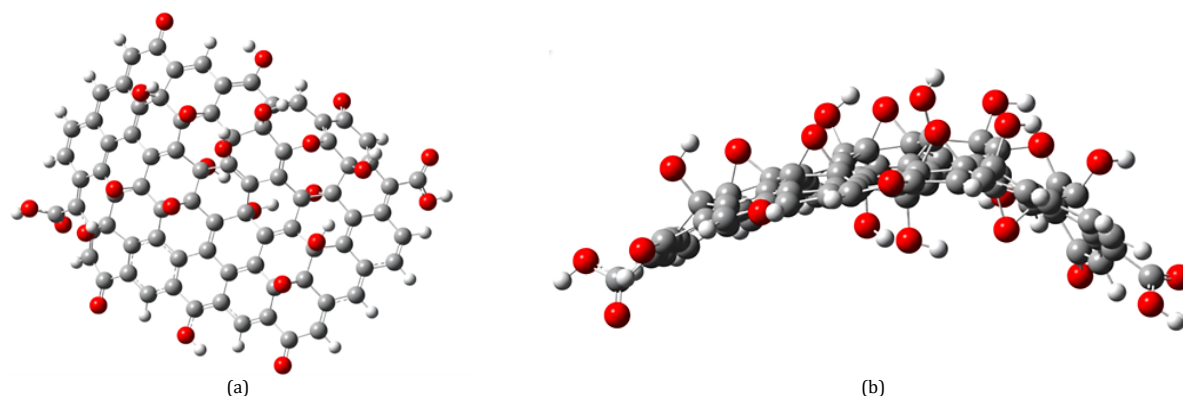
**Table 1.** Data of the composition and some electronic properties of the selected graphene oxide sheet model. The HOMO-LUMO gap ( $E_{\text{gap}}$ ) is in eV and the dipolar moment ( $\mu_D$ ) is in Debye.

C/O ratio	% Oxygen	(>C=O+OH)/CO <sub>2</sub> H ratio (at edge)	OH/epoxy ratio (at the main side)	$E_{\text{gap}}$ *	$\mu_D$
3.5	17	3	1.2	0.127	12.34

$$* E_{\text{gap}} = E_{\text{LUMO}} - E_{\text{HOMO}}$$

**Table 2.** Relevant bond lengths (Å) of the optimized geometry of PCT for the H<sub>2</sub>O solvent effect. (The percentages of accuracy with respect to the references considered are in parentheses.)

Reference/Bond	>C3-O11(H)	>C14-N12(H)	>C6-N12(H)	>C14-O15	O15...H10 (C5)
This work	1.371	1.357	1.413	1.233	2.237
Single crystal structure (X-ray) [41]	1.377 (0.44%)	1.340 (1.27%)	1.425 (0.84%)	1.232 (0.08%)	2.380
Theoretical [43]	1.382 (0.80%)	1.380 (1.67%)	1.416 (0.21%)	1.235 (0.16%)	2.199

**Figure 2.** (a) Top and (b) side view of the optimized geometry of graphene oxide.

On the basis of binding energy calculations of each model, the most stable one was selected for the subsequent adsorption studies; this model exhibited the highest dipole moment. Table 1 presents some data on its composition and electronic properties, such as the HOMO-LUMO gap ( $E_g$ ) and the dipolar moment ( $\mu_D$ ). Figure 2 shows the corresponding optimized geometry.

You can see in Figure 2 that additionally in this model, at the non-main side of the sheet (*trans* conformation), a combination of one epoxide group and two OH groups were added, as has been suggested [37]. It is important to note that the ratio C/O = 3.5 is only slightly higher than that reported by Gao *et al.* [38] (C/O = 2.44) and Quiao *et al.* [39] (C/O = 2.93), both of which are based on experimental data.

### 3.2. Reactivity of the graphene oxide sheet

Figure 3 shows the mapping of the frontier orbitals (HOMO and LUMO) and the molecular electrostatic potential map (MEP). Both frontier orbitals are showing that the available states correspond to a  $\pi$ -orbital conjugate system, which is extended over the same zone; therefore, these states facilitate a delocalized movement of the electronic charge, which could explain the very narrow HOMO-LUMO ( $E_{\text{gap}}$ ) gap observed in Table 2. This pattern observed in the HOMO and LUMO orbitals allows one to preserve a continuous domain of conjugate carbons (Figure 3), as has been suggested by Sinclair *et al.* [40], although a slight curvature is observed with respect to the pristine graphene sheet.

However, the MEP map displays orange and blue zones, which correspond to negative and positive charges, respectively. In the negative zones, epoxide and carbonyl groups are present, while in the positive ones, hydrogens belonging to hydroxyl groups are observed. It is anticipated that these two zones play a key role in the adsorption process. Finally, we report an average carbon-oxygen length of 1.42 Å in the epoxide groups, 1.33 Å for carbons bonded to the OH groups, and a C-O distance of 1.23 Å in the carbonyl groups.

### 3.3. Geometry and reactivity of the PCT molecule

Figure 4 shows the optimized geometry of PCT, revealing that is a flat molecule except for an out-of-plane methyl group. The most relevant characteristics of its geometry are a benzene ring with a hydroxyl group (phenolic fragment) forming a  $\pi$ -system and a polar acetamide group (-NH-CO-CH<sub>3</sub>) (amide fragment); both groups are substituted in the *para* position. In its crystalline form, PCT can exist mainly in two conformations due to the free rotation of the  $\sigma$ -bond. While one of the conformations has the -NH and -OH groups in the same direction, the other arranges them in opposite directions. According to the X-ray experiments of Haisa *et al.*, the first one is more stable in the crystalline phase and is the one presented in the two polymorphic forms [41,42]; in contrast, theoretical calculations made by Nguyen *et al.* [43] in both the gas phase and the solvent effect at the MP2/aug-cc-pVTZ level have presented the second one as the most stable conformation. The main reason is that both conformations have very similar geometries and therefore a slight energy difference of 0.288 kcal/mol. In this paper, the interaction of PCT with two solvents (water and formaldehyde) was studied, and it was found that the interaction ability was the same and was slightly more favored when the -NH and -OH groups pointed in opposite directions in both solvents.

Srivastava *et al.* [44] also considered the conformation with the -NH and -OH groups in opposite directions in their study of the interaction between PCT and oxalic acid. Finally, the negative value of the binding energy (BE = -2910.2 kcal/mol), calculated in the present work, indicated to us that this conformation is stable and was the one we used.

To validate the geometry of the PCT molecule obtained from our calculations, in Table 2, we are reporting the more relevant values of bond lengths compared with those reported by X-ray experiments of Haisa *et al.* [41] and the theoretical study of Nguyen *et al.* [43] in terms of percentages, which appear in parentheses. Notice that the values of bond lengths in this work agree with the experimental and theoretical reports, with an

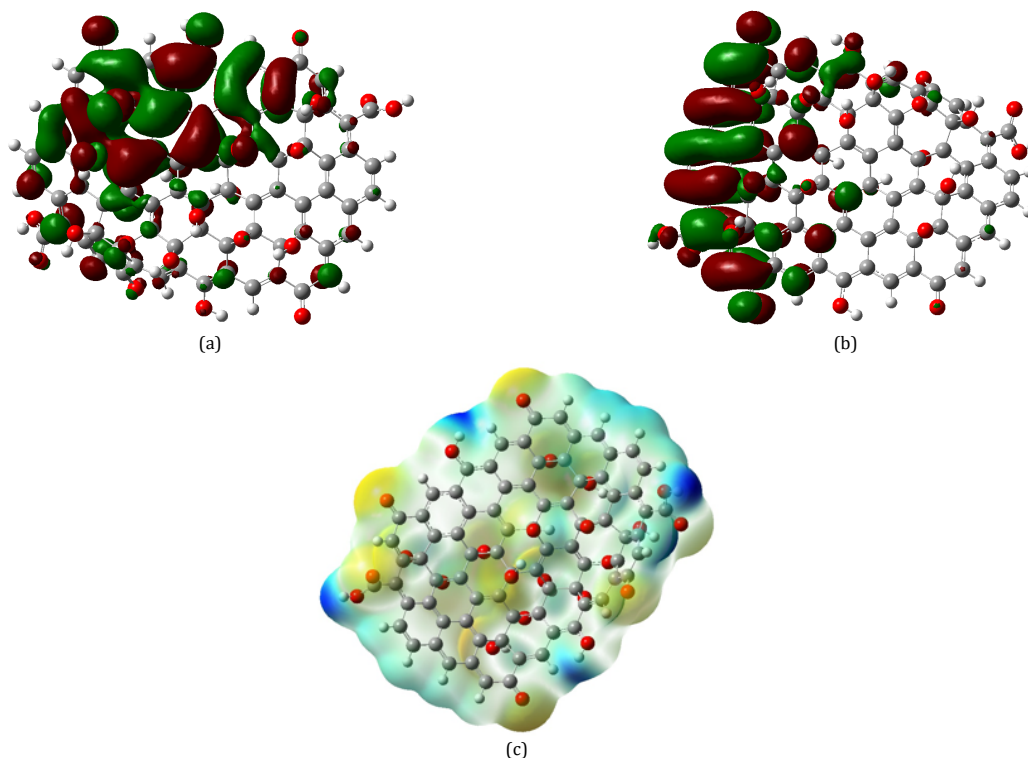


**Figure 3.** Mapping of the frontier orbitals (a, b) and MEP (c) (defined range from  $-8.108 \times 10^{-2}$  to  $8.108 \times 10^{-2}$ ) of the graphene oxide sheet. (a) HOMO orbital and (b) LUMO orbital.

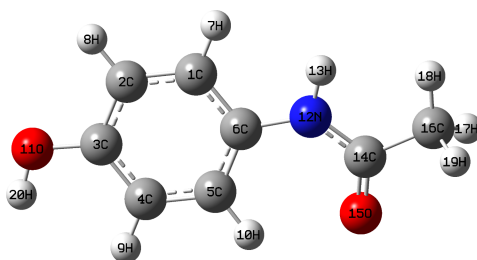


**Figure 4.** Optimized geometries of the PCT.

average error of less than 1%, except for the  $>\text{C}14\text{-N}12$  bond, which is slightly greater than 1%. The intramolecular hydrogen bond was not considered because it is a noncovalent interaction and not a chemical bond; however, these values are very close.

In relation to this non-covalent interaction involving the atoms  $>\text{C}=\text{O}15\cdots\text{H}10\text{-C}5$ , it should be noted that it is an intramolecular interaction mediated by aromatic hydrogens and therefore could not be considered an authentic hydrogen bond as it does not involve two electronegative atoms. Despite this, this kind of interaction will be essential in the adsorption processes, as will be seen later.

Figure 5 presents the HOMO-LUMO orbital maps and the MEP of the PCT molecule. Notice that (i) the frontier orbitals have a  $\pi$ -symmetry and (ii) the MEP map presents a very negative zone (in red) and two slightly negative zones (between green and orange), which correspond to the oxygens of the carbonyl group the OH- group, and the aromatic ring, respectively. Moreover, there is a very positive zone related to hydrogens belonging to N-H and O-H groups. Therefore, it is expected that the GO sheet can absorb the PCT through non-covalent interactions such as  $\pi$ -stacking and hydrogen bonds involving the -OH, -NH, and  $>\text{C}=\text{O}$  groups.

### 3.4. Study of the adsorption complexes PCT-GO

Taking into account the calculations for the GO and the PCT, the adsorption process was modeled considering four orientations for the approach of the PCT molecule on the GO sheet: (i) one of them, in parallel, to favor a possible stacking interaction between both conjugate systems (molecule-sheet), and (ii) three in a leaning position to favor the interaction of the  $>\text{C}=\text{O}$ , -OH, and -NH groups of the molecule with the sheet.

Figure 6 shows the optimized geometries of the orientation in parallel, with various interaction points labeled  $d_1, d_2, d_3$ , etc., where  $d_i$  represents each of the adsorption distances. For a better visualization of all the adsorption points between the PCT molecule and the GO sheet, Figure 6a shows one side of the PCT molecule, where the methyl group can be seen on the left, and Figure 6b shows the other side of the molecule, in which the methyl group can be seen on the right.

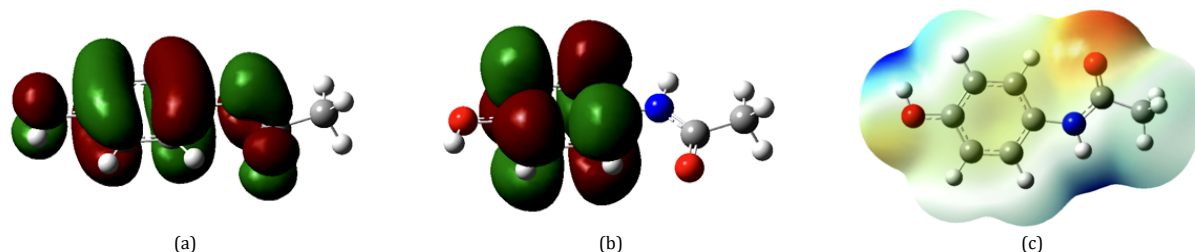
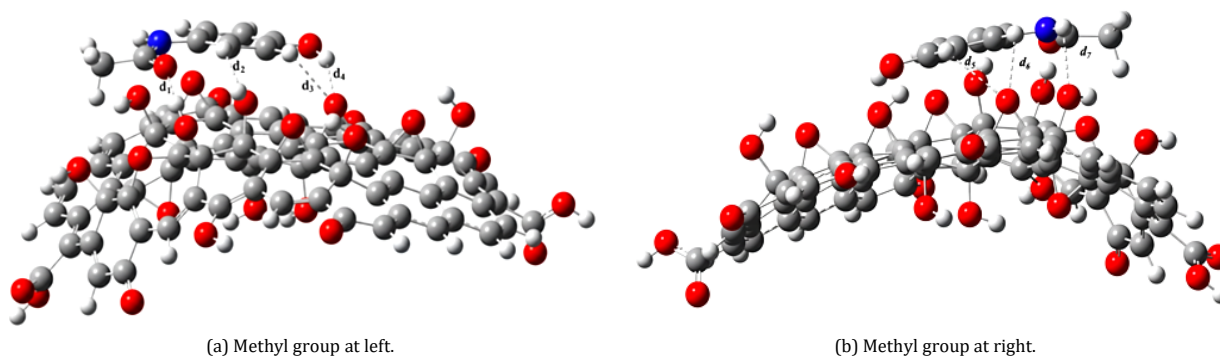
The adsorption distance values are depicted in Table 3. The distances  $d_1$  (1.84 Å) and  $d_4$  (2.07 Å) present the lower values and therefore come from the strongest interactions; These interactions correspond to conventional hydrogen bonds involving the lone pairs of the carbonyl and epoxy groups:  $>\text{C}=\text{O}\cdots\text{H-O}$  and  $\text{O-H}\cdots\text{O}_{\text{epox}}$  (the first group belongs to the PCT molecule and the second one to the GO sheet).



**Table 3.** Parameters for the adsorption complexes: adsorption energies ( $E_{\text{ads}}$ ) in kcal/mol, HOMO-LUMO-energy gap ( $E_{\text{gap}}$ ) in eV, and the adsorption distances ( $d_i$ ) in Å.

Orientations	$E_{\text{ads}}^*$	$E_{\text{gap}}$	Adsorption distances ( $d_i$ )			
In parallel (Figures 6a-6b)	21.662	-0.1272	$d_1 = 1.84$ $d_5 = 2.75$	$d_2 = 2.22$ $d_6 = 2.51$	$d_3 = 2.39$ $d_7 = 2.58$	$d_4 = 2.07$ -
Leaning position, entering through the carbonyl group of PCT (Figure 7a)	21.539	-0.1270	$d_1 = 2.05$	$d_2 = 2.11$	$d_3 = 2.53$	-
Leaning position, entering through the amine group of PCT (Figure 7b)	13.892	-0.1272	$d_1 = 2.02$	$d_2 = 2.82$	$d_3 = 2.23$	$d_4 = 2.80$

\* Calculated by:  $E_{\text{ads}} = [E_{\text{T}}(\text{GO sheet}) + E_{\text{T}}(\text{Paracetamol})] - E_{\text{T}}(\text{Adsorption complex})$ .

**Figure 5.** Mapping of frontier orbitals (a, b) and MEP (c) (defined range from  $-6.566 \times 10^{-2}$  to  $6.566 \times 10^{-2}$ ) of the PCT molecule; (a) HOMO orbital and (b) LUMO orbital.**Figure 6.** Optimized geometries of the adsorption complex in the parallel approach; (a) side of the PCT molecule where the methyl group is at left; (b) side of the PCT molecule where the methyl group is on the right.

The distances  $d_2$  (2.22 Å) and  $d_3$  (2.39 Å) correspond to non-covalent interactions mediated by aromatic hydrogens, which are characteristic of adsorption processes involving molecules such as the NSAID-type drugs in interaction with graphene-based sheets. These interactions involve the atoms:  $>\text{C}_{\text{arom}}-\text{H}_{\text{arom}} \cdots \text{O}-\text{H}$  and  $>\text{C}_{\text{arom}}-\text{H}_{\text{arom}} \cdots \text{O}_{\text{epox}}$ .

Another hydrogen bond at a  $d_7$  (2.58 Å) distance is observed between the amine and hydroxide groups:  $>\text{N}-\text{H} \cdots \text{O}-\text{H}$ . Finally, it can be seen two more distances,  $d_5$  (2.75 Å) and  $d_6$  (2.51 Å), that correspond to non-covalent interactions mediated by aromatic hydrogens involving  $>\text{C}_{\text{arom}}-\text{H}_{\text{arom}} \cdots \text{O}_{\text{epox}}$ . Interestingly, the position in parallel of the PCT molecule reinforced the intramolecular hydrogen bond mediated by aromatic hydrogen, observing 2.206 Å of bond distance, corresponding to a shortening of 0.031 Å.

Figures 7a and 7b show the two geometries obtained as a result of the approaching in leaning orientations by the carbonyl ( $>\text{C}=\text{O}$ ) and amine ( $>\text{NH}$ ) groups, respectively. In Figure 7a, the final position of the PCT molecule favored the interaction with both groups,  $>\text{C}=\text{O}$  and  $>\text{NH}$ ; you can see the presence of two hydrogen bonds with  $d_1$  (2.05 Å) and  $d_2$  (2.11 Å) distances, respectively, involving the atoms  $>\text{C}=\text{O} \cdots \text{H}-\text{O}$  and  $>\text{N}-\text{H} \cdots \text{O}_{\text{epox}}$  and besides, a weaker noncovalent interaction with a  $d_3$  (2.53 Å) distance mediated by methyl hydrogen:  $\text{C}_{\text{methyl}}-\text{H} \cdots \text{O}_{\text{epox}}$ . On the other hand, in Figure 7b, only a hydrogen bond with a distance of  $d_1$  (2.02 Å) involving the amine group was observed:  $>\text{N}-\text{H} \cdots \text{O}-\text{H}$ ; the other three non-covalent interactions were mediated by aromatic hydrogens, two of them with distances of  $d_2$  (2.82 Å) and  $d_4$  (2.80 Å), mediated by the atoms:  $>\text{C}_{\text{arom}}-\text{H}_{\text{arom}} \cdots \text{O}-\text{H}$ , and the third one, with a distance of  $d_3$  (2.23 Å), through the atoms:  $>\text{C}_{\text{arom}}-\text{H}_{\text{arom}} \cdots \text{O}_{\text{epox}}$ .

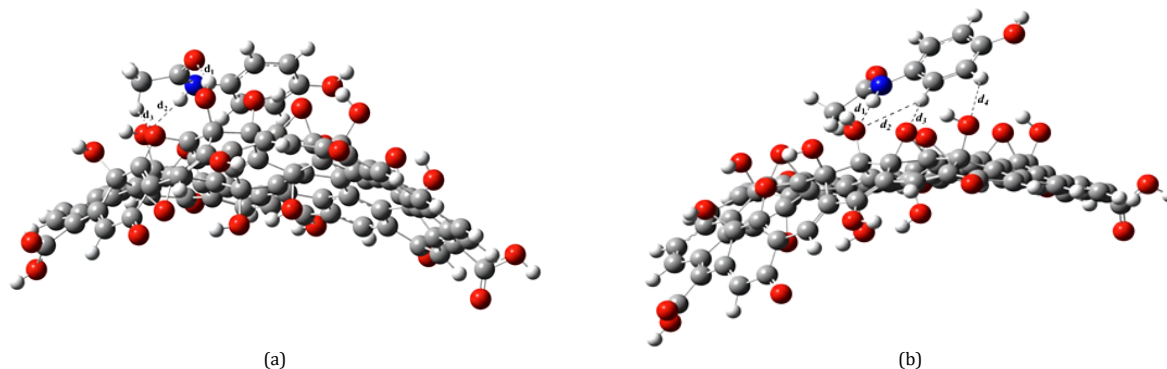
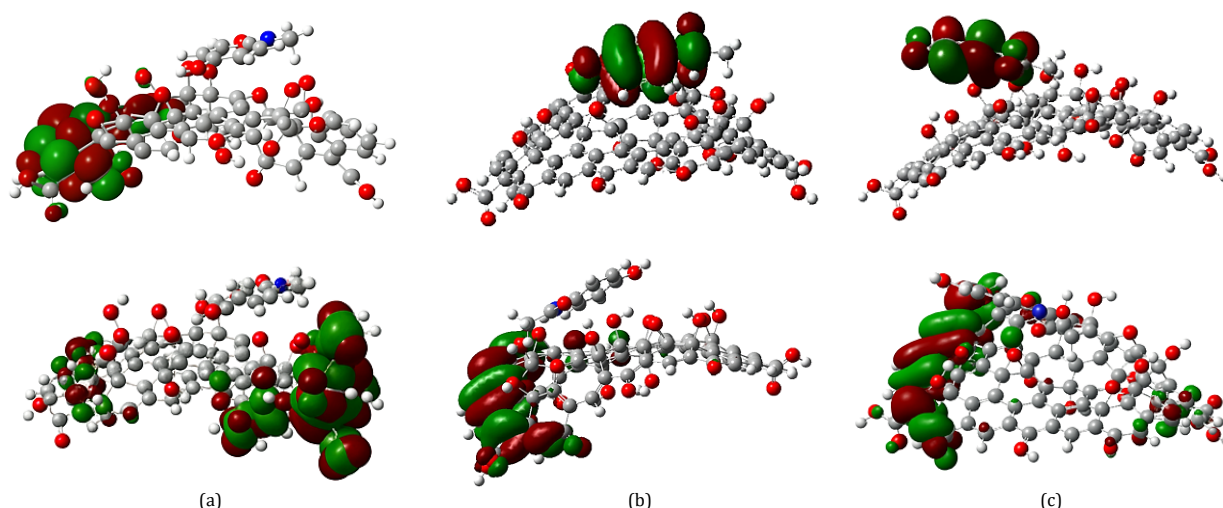
The values of the adsorption energies indicated that parallel orientations (Figure 6) and leaning, with a simultaneous interaction of the  $>\text{C}=\text{O}$  and  $-\text{NH}$  groups of the PCT molecule (Figure 7a), were the most favored. The orientation shown in Figure 7b, having the highest inclination, could only interact through a single  $>\text{NH}$  group of the PCT molecule. In both leaning orientations, the intramolecular hydrogen bond of the PCT molecule, mediated by an aromatic hydrogen, was weakened, with elongations of 0.05 Å and 0.08 Å in (a) and (b), respectively.

There are two aspects that should be highlighted: (i) the contribution of non-covalent interactions mediated by mostly aromatic hydrogens and also methyl hydrogens, with an arrangement very similar to that of a hydrogen bond and (ii) the interactions observed in the three adsorption complexes studied between the PCT molecule and the GO sheet corresponded to adsorption distances of less than 3.00 Å and adsorption energies above 10 kcal/mol (22 and 13 kcal/mol), which allow us to establish that the adsorption process of PCT over GO corresponds to a chemisorption.

Figure 8 presents the mapping of the frontier orbitals (HOMO and LUMO) for the three adsorption complexes, where it can be observed that only  $\pi$ -orbitals are present. However, while the adsorption complex with the PCT molecule in parallel (Figure 6) maintains its frontier orbitals within the GO sheet, for the complexes C and D, the HOMO orbital appears on the PCT molecule and the LUMO orbital on the GO sheet. Therefore, it can be expected in (A/B) a tendency to move the electronic charge over the surface, while the entry of the molecule in an inclined orientation (C and D) could favor a movement of electronic charges from the molecule to the surface.

**Table 4.** Percentages of elongation of the bonds in the PCT molecule during the adsorption process.

Bond	Complex (A/B)	Complex (C)	Complex (D)
C14(>C=O)-N12(-NH)	2.06	1.98	1.71
C <sub>arom</sub> - C <sub>arom</sub>	0.38	0.38	-
C <sub>arom</sub> - N12 (-NH)	0.30	0.17	0.20
C <sub>arom</sub> - O11 (OH)	0.45	0.46	0.65

**Figure 7.** Optimized geometries of the adsorption complex with leaning orientation: (a) favoring the interaction with the carbonyl and -NH groups and (b) favoring the interaction with the -NH groups.**Figure 8.** Mapping of the HOMO-LUMO frontier orbitals for the adsorption complexes: (a) in parallel orientation, (b), and (c) in leaning orientation (HOMO orbitals appear on the top figure, and LUMO orbitals on the lower).

In summary, the adsorption energies for the most preferred adsorption complexes were 22 kcal/mol with adsorption distances between 1.84 and 2.60 Å. These values agree with those of other studies. For example, Gonzalez-Rodriguez *et al.* [45] used a DFT formalism to study the adsorption of five drugs, such as atrazine, caffeine, carbamazepine, sulfamethoxazole, and ibuprofen, onto activated carbon, and the adsorption energies were between 17 and 26 kcal/mol. Also, Hasanzade *et al.* [46] studied the adsorption of the thioguanine drug on the surface of graphene oxide using the DFT approach with M06-2X/6-31G\*\*, the same functional used in this work, together with molecular dynamics and solvent effect; they found an adsorption process highly favored with adsorption energies from 10.04 to 26.70 kcal/mol; likewise, the most favored adsorption complex, in which the Thioguanine molecule was located in parallel to the GO nanosheet, exhibited adsorption distances between 1.90 and 2.26 Å. Anchique *et al.* [47] studied the adsorption of ibuprofen over a GO model with structure type-coronene and DFT with a theory level of  $\omega$ B97X-D/6-311G(2d,p) and reported an adsorption energy of 19.41 kcal/mol. Finally, Matos *et al.* [48] performed periodic DFT calculations with an LDA functional of the PCT adsorption over

three models of GO, considering the epoxy group, the -OH group, and the carboxyl group separately; the adsorption energies gave values in a higher range, between 7.84 and 45.66 kcal/mol, due to the structural diversity of the three GO models considered. All of these studies confirm that the DFT approach followed in this work and the GO sheet modeled were suitable.

### 3.5. Contribution of the adsorption process to the degradation of PCT

To assess the potential of the PCT adsorption on the GO sheet for promoting the degradation of this drug, Table 4 presents some relevant percentages of bond elongation in the PCT molecule, calculated from the bond distances before and after the adsorption process. As explained below, these changes could be related to some fragmentation patterns of this molecule.

Belal *et al.* [49] used a gas chromatograph coupled with a mass spectrometer (GC-MS) to obtain a mass spectrum of the PCT molecule with  $m/z$  peaks at 134, 122, 109, 94, 80, 63, 52, and 43. Starting from the molecular peak ( $M^+$ ) at  $m/z = 151$ , the cleavage of the bond C14-N12 can produce two alternative

fragmentation routes. The first one initiates with the formation of the base peak at  $m/z = 109$  by the hydrogen transfer from the methyl group to the nitrogen, followed by the loss of the ketene group ( $\text{CH}_2=\text{C}=\text{O}$ ), which, after protonation, forms the fragment at  $m/z = 43$ . From the base peak, the cleavage of two  $\text{C}_{\text{arom}}-\text{C}_{\text{arom}}$  bonds produces the loss of the  $-\text{COH}$  radical and the formation of a cyclopentadienylidene ammonium cation at  $m/z = 80$ . The second one involves hydrogen transfer from the methyl group to the carbonyl group, followed by the migration of the  $\text{CH}_2$  group to nitrogen and the loss of the  $-\text{COH}$  radical to form a fragment at  $m/z = 122$ , which can produce a fragment at  $m/z = 94$  by the cleavage of  $\text{C}_{\text{arom}}-\text{N}(\text{NH})$  bond, followed by the cleavage of two  $\text{C}_{\text{arom}}-\text{C}_{\text{arom}}$  bonds originating the loss of the  $-\text{CH}-\text{COH}$  species to form a fragment at  $m/z = 52$ . At the final stage, directly from the molecular peak, the cleavage of the  $\text{C}_{\text{arom}}-\text{O}(\text{OH})$  bond and consequently the exit of the  $\text{OH}$  radical, to form a fragment at  $m/z = 134$ , followed by the cleavage of two  $\text{C}_{\text{arom}}-\text{C}_{\text{arom}}$  bonds and the loss of the  $-\text{CH}_3-\text{CO}-\text{N}=\text{CH}_2$  species to generate a fragment at  $m/z = 63$ . The analysis described above has confirmed that the adsorption process of PCT over a GO sheet can contribute to weakening certain bonds in the molecule related to its fragmentation. Therefore, these adsorption processes mediated by GO sheets could contribute to PCT degradation.

#### 4. Conclusions

In this study, the adsorption energies and interaction distances of the paracetamol-graphene oxide (PCT-GO) adsorption complex were estimated. The calculations suggest that the adsorption process of PCT on GO is primarily favored by chemisorption. The main interactions involved in this chemisorption process were a stacking interaction between both conjugate systems (molecule-sheet); the hydrogen bonds involving the carbonyl,  $-\text{OH}$ , and  $>\text{NH}$  groups of the molecule together with the  $-\text{OH}$  and epoxy groups of the GO sheet; finally, the noncovalent interactions mediated by aromatic and also methyl hydrogens, with an arrangement very similar to that of a hydrogen bond. In this way, it can be confirmed that the heterogeneity of the GO sheet, due to the functional groups regulated by parameters such as the C/O ratio and the oxygen percentage, has a strong influence on its adsorption capacity and stability. This theoretical study has confirmed that GO can act as an effective adsorbent material for the PCT molecule, contributing to its degradation. Therefore, the GO sheets could be tested as an interesting adsorbent material to be included in existing hybrid methodologies to remove emergent contaminants from water and thus further improve its quality.

#### Acknowledgements

We gratefully acknowledge the generous computing time provided by Dirección General de Comunicación at the Universidad Nacional Autónoma de México (DG TIC- UNAM) through the Grants LANCAD-UNAM-DGTIC-156. This research was supported by a grant from the "Cátedra de Investigación C12448"-FES-Cuautitlán-UNAM.

#### Disclosure statement

Conflict of interest: The authors declare that they have no financial interest/personal relationships which may be considered as potential competing interests.  
Ethical approval: All ethical guidelines have been followed.

#### CRedit authorship contribution statement

Conceptualization: Esther Agacino-Valdés; Formal Analysis: Esther Agacino Valdés, Beatriz Paulina López-Jesús, Sandy-María Pacheco-Ortín; Investigation: Esther Agacino Valdés, Beatriz Paulina López-Jesús, Sandy-María Pacheco-Ortín; Writing - Original Draft: Esther Agacino Valdés, Sandy-María Pacheco-Ortín; Writing - Review and Editing: Esther Agacino Valdés,

Beatriz P. López-Jesús; Visualization: Beatriz P. López-Jesús; Supervision: Esther Agacino-Valdés.

#### ORCID and Email

Beatriz Paulina López-Jesús

[paulinaloje27@gmail.com](mailto:paulinaloje27@gmail.com)

<https://orcid.org/0009-0002-4769-1884>

Sandy María Pacheco-Ortín

[sandymaria@cuautitlan.unam.mx](mailto:sandymaria@cuautitlan.unam.mx)

<https://orcid.org/0000-0003-2477-1101>

Esther Agacino Valdés

[eagacino@unam.mx](mailto:eagacino@unam.mx)

<https://orcid.org/0000-0002-5386-8933>

#### References

- [1]. Luo, Y.; Guo, W.; Ngo, H. H.; Nghiem, L. D.; Hai, F. I.; Zhang, J.; Liang, S.; Wang, X. C. A review on the occurrence of micropollutants in the aquatic environment and their fate and removal during wastewater treatment. *Sci. Total. Environ.* **2014**, 473-474, 619-641.
- [2]. Surana, D.; Gupta, J.; Sharma, S.; Kumar, S.; Ghosh, P. A review on advances in removal of endocrine disrupting compounds from aquatic matrices: Future perspectives on utilization of agri-waste based adsorbents. *Sci. Total. Environ.* **2022**, 826, 154129.
- [3]. Kumar, R.; Qureshi, M.; Vishwakarma, D. K.; Al-Ansari, N.; Kuriqi, A.; Elbeltagi, A.; Saraswat, A. A review on emerging water contaminants and the application of sustainable removal technologies. *Case Stud. Chem. Environ. Eng.* **2022**, 6, 100219.
- [4]. Feng, L.; van Hullebusch, E. D.; Rodrigo, M. A.; Esposito, G.; Oturan, M. A. Removal of residual anti-inflammatory and analgesic pharmaceuticals from aqueous systems by electrochemical advanced oxidation processes. A review. *Chem. Eng. J.* **2013**, 228, 944-964.
- [5]. Veras, T. B.; Luiz Ribeiro de Paiva, A.; Duarte, M. M.; Napoleão, D. C.; da Silva Pereira Cabral, J. J. Analysis of the presence of anti-inflammatory drugs in surface water: A case study in Beberibe river - PE, Brazil. *Chemosphere* **2019**, 222, 961-969.
- [6]. Phong Vo, H. N.; Le, G. K.; Hong Nguyen, T. M.; Bui, X.; Nguyen, K. H.; Rene, E. R.; Vo, T. D.; Thanh Cao, N.; Mohan, R. Acetaminophen micropollutant: Historical and current occurrences, toxicity, removal strategies and transformation pathways in different environments. *Chemosphere* **2019**, 236, 124391.
- [7]. Pacheco-Álvarez, M.; Picos Benítez, R.; Rodríguez-Narváez, O. M.; Brillas, E.; Peralta-Hernández, J. M. A critical review on paracetamol removal from different aqueous matrices by Fenton and Fenton-based processes, and their combined methods. *Chemosphere* **2022**, 303, 134883.
- [8]. Valdez-Carrillo, M.; Abrell, L.; Ramírez-Hernández, J.; Reyes-López, J. A.; Carreón-Díazconti, C. Pharmaceuticals as emerging contaminants in the aquatic environment of Latin America: a review. *Environ. Sci. Pollut. Res.* **2020**, 27 (36), 44863-44891.
- [9]. Jiang, T.; Wu, W.; Ma, M.; Hu, Y.; Li, R. Occurrence and distribution of emerging contaminants in wastewater treatment plants: A globally review over the past two decades. *Sci. Total. Environ.* **2024**, 951, 175664.
- [10]. Lee, W. J.; Goh, P. S.; Lau, W. J.; Ismail, A. F. Removal of Pharmaceutical Contaminants from Aqueous Medium: A State-of-the-Art Review Based on Paracetamol. *Arab. J. Sci. Eng.* **2020**, 45 (9), 7109-7135.
- [11]. Salimi, M.; Esrafil, A.; Gholami, M.; Jonidi Jafari, A.; Rezaei Kalantary, R.; Farzadkia, M.; Kermani, M.; Sobhi, H. R. Contaminants of emerging concern: a review of new approach in AOP technologies. *Environ. Monit. Assess.* **2017**, 189 (8), 414 <https://doi.org/10.1007/s10661-017-6097-x>.
- [12]. Leyva, E.; Moctezuma, E.; Baines, K. M.; Noriega, S.; Zarazua, E. A Review on Chemical Advanced Oxidation Processes for Pharmaceuticals with Paracetamol as a Model Compound. Reaction Conditions, Intermediates and Total Mechanism. *Curr. Org. Chem.* **2018**, 22 (1), 2-17.
- [13]. Yang, W.; Zhou, H.; Cicek, N. Treatment of Organic Micropollutants in Water and Wastewater by UV-Based Processes: A Literature Review. *Crit. Rev. Environ. Sci. Technol.* **2014**, 44 (13), 1443-1476.
- [14]. Checa, M.; Beltrán, F. J.; Rivas, F. J.; Cordero, E. On the role of a graphene oxide/titania catalyst, visible LED and ozone in removing mixtures of pharmaceutical contaminants from water and wastewater. *Environ. Sci. Water Res. Technol.* **2020**, 6 (9), 2352-2364.
- [15]. Moussavi, G.; Hossaini, Z.; Pourakbar, M. High-rate adsorption of acetaminophen from the contaminated water onto double-oxidized graphene oxide. *Chem. Eng. J.* **2016**, 287, 665-673.
- [16]. Scaria, J.; Gopinath, A.; Ranjith, N.; Ravindran, V.; Ummar, S.; Nidheesh, P.; Kumar, M. S. Carbonaceous materials as effective adsorbents and



- catalysts for the removal of emerging contaminants from water. *J. Cleaner. Prod.* **2022**, 350, 131319.
- [17]. Almeida-Naranjo, C. E.; Guerrero, V. H.; Villamar-Ayala, C. A. Emerging Contaminants and Their Removal from Aqueous Media Using Conventional/Non-Conventional Adsorbents: A Glance at the Relationship between Materials, Processes, and Technologies. *Water* **2023**, 15 (8), 1626.
- [18]. Anegebe, B.; Ifijen, I. H.; Maliki, M.; Uwidia, I. E.; Aigbodion, A. I. Graphene oxide synthesis and applications in emerging contaminant removal: a comprehensive review. *Environ. Sci. Eur.* **2024**, 36 (1), 1–34 <https://doi.org/10.1186/s12302-023-00814-4>.
- [19]. Chen, H.; Gao, B.; Li, H. Removal of sulfamethoxazole and ciprofloxacin from aqueous solutions by graphene oxide. *J. Hazard. Mater.* **2015**, 282, 201–207.
- [20]. Lee, B. C.; Lim, F. Y.; Loh, W. H.; Ong, S. L.; Hu, J. Emerging Contaminants: An Overview of Recent Trends for Their Treatment and Management Using Light-Driven Processes. *Water* **2021**, 13 (17), 2340.
- [21]. López Zavala, M.; Jaber Lara, C. R. Degradation of Paracetamol and Its Oxidation Products in Surface Water by Electrochemical Oxidation. *Environ. Eng. Sci.* **2018**, 35 (11), 1248–1254.
- [22]. Kong, E.; Chau, J.; Lai, C.; Khe, C.; Sharma, G.; Kumar, A.; Siengchin, S.; Sanjay, M. GO/TiO<sub>2</sub>-Related Nanocomposites as Photocatalysts for Pollutant Removal in Wastewater Treatment. *Nanomaterials* **2022**, 12 (19), 3536.
- [23]. Guo, S.; Zhang, G.; Guo, Y.; Yu, J. C. Graphene oxide-Fe<sub>2</sub>O<sub>3</sub> hybrid material as highly efficient heterogeneous catalyst for degradation of organic contaminants. *Carbon* **2013**, 60, 437–444.
- [24]. Frisch, M. J.; Trucks, G. W.; Schlegel, H. B.; Scuseria, G. E.; Robb, M. A.; Cheeseman, J. R.; Montgomery, J. A.; Vreven, T.; Kudin, K. N.; Burant, J. C.; Millam, J. M.; Iyengar, S. S.; Tomasi, J.; Barone, V.; Mennucci, B.; Cossi, M.; Scalmani, G.; Rega, N.; Petersson, G. A.; Nakatsuji, H.; Hada, M.; Ehara, M.; Toyota, K.; Fukuda, R.; Hasegawa, J.; Ishida, M.; Nakajima, T.; Honda, Y.; Kitao, O.; Nakai, H.; Klene, M.; Li, X.; Knox, J. E.; Hratchian, H. P.; Cross, J. B.; Adamo, C.; Jaramillo, J.; Gomperts, R.; Stratmann, R. E.; Yazyev, O.; Austin, A. J.; Cammi, R.; Pomelli, C.; Ochterski, J. W.; Ayala, P. Y.; Morokuma, K.; Voth, G. A.; Salvador, P.; Dannenberg, J. J.; Zakrzewski, V. G.; Dapprich, S.; Daniels, A. D.; Strain, M. C.; Farkas, O.; Malick, D. K.; Rabuck, A. D.; Raghavachari, K.; Foresman, J. B.; Ortiz, J. V.; Cui, Q.; Baboul, A. G.; Clifford, S.; Cioslowski, J.; Stefanov, B. B.; Liu, G.; Liashenko, A.; Piskorz, P.; Komaromi, I.; Martin, R. L.; Fox, D. J.; Keith, T.; Al-Laham, M. A.; Peng, C. Y.; Nanayakkara, A.; Challacombe, M.; Gill, P. M. W.; Johnson, B.; Chen, W.; Wong, M. W.; Gonzalez, C.; Pople, J. A. Gaussian, Inc., Wallingford CT, 2009.
- [25]. Zhao, Y.; Truhlar, D. G. A new local density functional for main-group thermochemistry, transition metal bonding, thermochemical kinetics, and noncovalent interactions. *J. Chem. Phys.* **2006**, 125 (19), 194101 <https://doi.org/10.1063/1.2370993>.
- [26]. Zhao, Y.; Truhlar, D. G. The M06 suite of density functionals for main group thermochemistry, thermochemical kinetics, noncovalent interactions, excited states, and transition elements: two new functionals and systematic testing of four M06-class functionals and 12 other functionals. *Theor. Chem. Acc.* **2007**, 120 (1-3), 215–241.
- [27]. Vovusha, H.; Sanyal, S.; Sanyal, B. Interaction of Nucleobases and Aromatic Amino Acids with Graphene Oxide and Graphene Flakes. *J. Phys. Chem. Lett.* **2013**, 4 (21), 3710–3718.
- [28]. Safdari, F.; Raissi, H.; Shahabi, M.; Zaboli, M. DFT Calculations and Molecular Dynamics Simulation Study on the Adsorption of 5-Fluorouracil Anticancer Drug on Graphene Oxide Nanosheet as a Drug Delivery Vehicle. *J. Inorg. Organomet. Polym.* **2017**, 27 (3), 805–817.
- [29]. Rohini, K.; Sylvinson, D. M.; Swathi, R. S. Intercalation of HF, H<sub>2</sub>O, and NH<sub>3</sub> Clusters within the Bilayers of Graphene and Graphene Oxide: Predictions from Coronene-Based Model Systems. *J. Phys. Chem. A.* **2015**, 119 (44), 10935–10945.
- [30]. Zaboli, M.; Raissi, H.; Moghaddam, N. R.; Farzad, F. Probing the adsorption and release mechanisms of cytarabine anticancer drug on/from dopamine functionalized graphene oxide as a highly efficient drug delivery system. *J. Mol. Liq.* **2020**, 301, 112458.
- [31]. Shahabi, M.; Raissi, H. Investigation of the solvent effect, molecular structure, electronic properties and adsorption mechanism of Tegafur anticancer drug on Graphene nanosheet surface as drug delivery system by molecular dynamics simulation and density functional approach. *J. Incl. Phenom. Macrocycl. Chem.* **2017**, 88 (3-4), 159–169.
- [32]. Marenich, A. V.; Cramer, C. J.; Truhlar, D. G. Universal Solvation Model Based on Solute Electron Density and on a Continuum Model of the Solvent Defined by the Bulk Dielectric Constant and Atomic Surface Tensions. *J. Phys. Chem. B.* **2009**, 113 (18), 6378–6396.
- [33]. Velázquez-López, L.; Pacheco-Ortín, S.; Mejía-Olvera, R.; Agacino-Valdés, E. DFT study of CO adsorption on nitrogen/boron doped-graphene for sensor applications. *J. Mol. Model.* **2019**, 25 (4), 91 <https://doi.org/10.1007/s00894-019-3973-z>.
- [34]. Yeamin, M. B.; Faginas-Lago, N.; Albertí, M.; Cuesta, I. G.; Sánchez-Marín, J.; Sánchez de Merás, A. M. Multi-scale theoretical investigation of molecular hydrogen adsorption over graphene: coronene as a case study. *RSC. Adv.* **2014**, 4 (97), 54447–54453.
- [35]. Lerf, A. 13C and 1H MAS NMR Studies of Graphite Oxide and Its Chemically Modified Derivatives. *Solid State Ion.* **1997**, 101–103, 857–862.
- [36]. Lerf, A.; He, H.; Forster, M.; Klinowski, J. Structure of Graphite Oxide Revisited. *J. Phys. Chem. B.* **1998**, 102 (23), 4477–4482.
- [37]. Luo, H.; Auchterlonie, G.; Zou, J. A thermodynamic structural model of graphene oxide. *J. Appl. Phys.* **2017**, 122 (14), 145101 <https://doi.org/10.1063/1.4991967>.
- [38]. Gao, W.; Alemany, L. B.; Ci, L.; Ajayan, P. M. New insights into the structure and reduction of graphite oxide. *Nature Chem.* **2009**, 1 (5), 403–408.
- [39]. Qiao, Q.; Liu, C.; Gao, W.; Huang, L. Graphene oxide model with desirable structural and chemical properties. *Carbon* **2019**, 143, 566–577.
- [40]. Sinclair, R. C.; Coveney, P. V. Modeling Nanostructure in Graphene Oxide: Inhomogeneity and the Percolation Threshold. *J. Chem. Inf. Model.* **2019**, 59 (6), 2741–2745.
- [41]. Haisa, M.; Kashino, S.; Kawai, R.; Maeda, H. The Monoclinic Form of p-Hydroxyacetanilide. *Acta. Crystallogr. B. Struct. Crystallogr. Cryst. Chem.* **1976**, 32 (4), 1283–1285.
- [42]. Haisa, M.; Kashino, S.; Maeda, H. The Orthorhombic Form of P-Hydroxyacetanilide. *Acta Crystallogr. B* **1974**, 30 (10), 2510–2512.
- [43]. Nguyen, T. H.; Nguyen, T. H.; Le, T. T.; Vu Dang, H.; Nguyen, H. M. Interactions between Paracetamol and Formaldehyde: Theoretical Investigation and Topological Analysis. *ACS. Omega* **2023**, 8 (13), 11725–11735.
- [44]. Srivastava, K.; Shimpi, M. R.; Srivastava, A.; Tandon, P.; Sinha, K.; Velago, S. P. Vibrational analysis and chemical activity of paracetamol-oxalic acid cocrystal based on monomer and dimer calculations: DFT and AIM approach. *RSC. Adv.* **2016**, 6 (12), 10024–10037.
- [45]. González-Rodríguez, L.; Yáñez, O.; Mena- Ulecia, K.; Hidalgo-Rosa, Y.; García- Carmona, X.; Ulloa- Tesser, C. Exploring the adsorption of five emerging pollutants on activated carbon: A theoretical approach. *J. Environ. Chem. Eng.* **2024**, 12 (3), 112911.
- [46]. Hasanazade, Z.; Raissi, H. Solvent/co-solvent effects on the electronic properties and adsorption mechanism of anticancer drug Thioguanine on Graphene oxide surface as a nanocarrier: Density functional theory investigation and a molecular dynamics. *Appl. Surf. Sci.* **2017**, 422, 1030–1041.
- [47]. Anchique, L.; Alcázar, J. J.; Ramos-Hernandez, A.; Méndez-López, M.; Mora, J. R.; Rangel, N.; Paz, J. L.; Márquez, E. Predicting the Adsorption of Amoxicillin and Ibuprofen on Chitosan and Graphene Oxide Materials: A Density Functional Theory Study. *Polymers* **2021**, 13 (10), 1620.
- [48]. de Matos, C. F.; Leão, M. B.; Vendrame, L. F.; Jauris, I. M.; Zanella, I.; Fagan, S. B. Unlocking the paracetamol adsorption mechanism in graphene tridimensional-based materials: an experimental-theoretical approach. *Front. Carbon* **2024**, 3, 1305183 <https://doi.org/10.3389/frcarb.2024.1305183>.
- [49]. Belal, T.; Awad, T.; Clark, R. Determination of Paracetamol and Tramadol Hydrochloride in Pharmaceutical Mixture Using HPLC and GC-MS. *J. Chromatogr. Sci.* **2009**, 47 (10), 849–854.



Copyright © 2025 by Authors. This work is published and licensed by Atlanta Publishing House LLC, Atlanta, GA, USA. The full terms of this license are available at <https://www.eurchem.com/index.php/eurchem/terms> and incorporate the Creative Commons Attribution-Non Commercial (CC BY NC) (International, v4.0) License (<http://creativecommons.org/licenses/by-nc/4.0>). By accessing the work, you hereby accept the Terms. This is an open access article distributed under the terms and conditions of the CC BY NC License, which permits unrestricted non-commercial use, distribution, and reproduction in any medium, provided the original work is properly cited without any further permission from Atlanta Publishing House LLC (European Journal of Chemistry). No use, distribution, or reproduction is permitted which does not comply with these terms. Permissions for commercial use of this work beyond the scope of the License (<https://www.eurchem.com/index.php/eurchem/terms>) are administered by Atlanta Publishing House LLC (European Journal of Chemistry).